

# Polymer wedge for perfectly vertical light coupling to silicon

J. Schrauwen, S. Scheerlinck, D. Van Thourhout, R. Baets

## ABSTRACT

We present the design and fabrication of a refractive polymer wedge that allows perfectly vertical coupling of light into a silicon waveguide, which is of interest for flip-chip bonding of vertical cavity emitting light sources on a silicon integrated circuit. The structure includes a conventional diffractive grating coupler that requires off-normal incidence to avoid second order Bragg reflections. The polymer wedge is thus used to refract vertically impinging light into an off-normal wave that couples into the underlying grating. The fabrication involves two steps: mold fabrication and imprint replication. Firstly negative wedge-shaped craters are etched into a quartz mold by Focused-ion-beam milling. Secondly the mold is used to imprint a UV-curable polymer onto a silicon chip containing waveguides and grating couplers, and so replicating the wedges. The characterization setup consisted of a fiber-to-fiber transmission measurement of a silicon waveguide equipped with a pair of grating couplers and polymer wedges. The obtained fiber coupling efficiency was equal to the efficiency of regular grating couplers and fiber positioned at an off-normal angle. The proposed fabrication method enables low cost integration of vertical cavity emitting light sources on silicon integrated photonic circuits.

**Keywords:** Refraction, grating coupler, Bragg, silicon-on-insulator, focused-ion-beam, imprint, VCSEL

## 1. INTRODUCTION

One of the problems of a high index contrast platform for integrated optical circuits such as silicon-on-insulator (SOI) is the difficulty of coupling between the tightly confined silicon optical mode (with typical dimensions of  $200 \text{ nm} \times 500 \text{ nm}$ ) and the relatively large mode in a standard single mode optical fiber (typically  $10 \mu\text{m} \times 10 \mu\text{m}$ ). Several in-plane approaches with low losses were proposed such as inverted tapers and three dimensional tapers. However, out-of-plane coupling with diffractive gratings is attractive because the optical mode can be accessed anywhere on the wafer, which enables wafer-scale testing; furthermore they make facet polishing unnecessary. Due to the high index contrast in the SOI platform, gratings can be made reasonably efficient and compact.<sup>1</sup> As depicted in Fig. 1 it is advantageous to use a nearly second order grating to avoid reflections but still exploit out-of-plane diffraction. The conventional grating design consists of shallowly etched rectangular trenches in a broad silicon waveguide. However, the approach of vertically coupling with a diffractive grating has several inconveniences, some of which have been solved recently. A first inconvenience is the limited efficiency of coupling fiber and silicon waveguide modes. This was recently addressed by incorporating a metal bottom reflector,<sup>2</sup> by using a thicker silicon membrane in the grating area<sup>3</sup> or by etching slanted slits.<sup>4</sup> A second inconvenience is the need for an adiabatic taper that is typically  $500 \mu\text{m}$  long. Recently the use of focusing grating structures was reported, reducing the taper length to less than  $70 \mu\text{m}$  without efficiency penalty.<sup>5</sup>

The final inconvenience is the need for near-vertical coupling to avoid reflections while coupling in and out of the silicon integrated circuit. If a grating would be designed for perfectly vertical coupling, the second Bragg diffraction order would cause large reflections. This can partially be overcome by using a thin slit adjacent to the grating, with the purpose of achieving destructive interference for the second order Bragg reflection, as was theoretically shown.<sup>6</sup> However, this approach is not completely satisfactory because reflections are only canceled in a narrow wavelength range. Perfectly vertical coupling potentially opens opportunities for bonding of vertically emitting III-V sources and simplifies packaging and wafer-scale diagnostics.

In this paper we present design and fabrication of a polymer wedge to refract the first Bragg diffraction order to a vertical wave that couples to a vertically positioned fiber, and vice versa. The principle is shown in Fig. 2. Reflections are avoided due to the near-vertical Bragg diffraction. The polymer wedges were fabricated

---

Further author information: (Send correspondence to J. Schrauwen)

E-mail: jonathan.schrauwen@intec.ugent.be, Telephone: +32(0)9264 8933, Address: Photonics Research Group, Department of Information technology, Ghent University - IMEC, Sint-Pietersnieuwstraat 41, 9000 Gent, Belgium

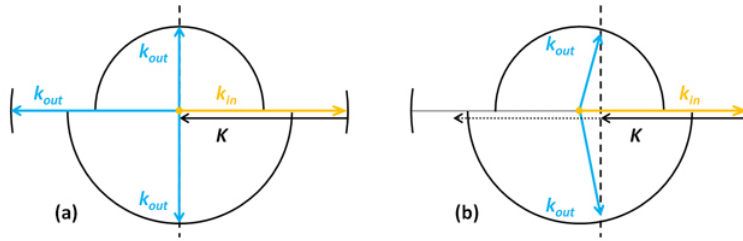


Figure 1. Bragg diffraction diagrams for incoming light with  $k$ -vector  $k_{in}$  and grating with reciprocal period  $K$ : (a) for a second order grating there is reflection in the waveguide; (b) by choosing e.g. a slightly longer grating period the second order reflection is avoided but the out-of-plane diffraction remains.

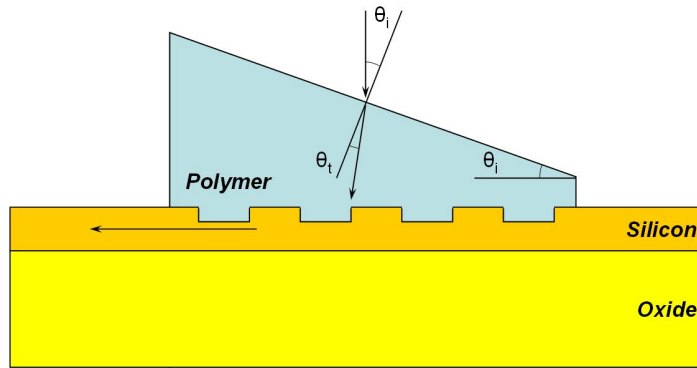


Figure 2. Principle of a polymer grating wedge: vertically incident light is refracted to near-vertical incidence, which is optimal for coupling with low reflections into a silicon waveguide.

by imprint lithography of a FIB fabricated mold as described later. This procedure is suited for wafer scale fabrication of devices and enables flip-chip bonding of VCSELs on photonic integrated circuits. The approach of bonding of finished III-V devices is currently being used in industry to provide light sources on passive material platforms such as silicon, nitride or silica. However, the coupling (usually of horizontal cavity lasers) often requires slanted edges or angled mirrors that can not be fabricated with typical high-volume fabrication technologies. The technique presented in this paragraph envisages the use of VCSELs that inherently emit perfectly vertically and do not require extra mirrors or facets. The polymer wedge and grating couple this perfectly vertical light into the silicon circuit without reflections. Due to the compatibility with high volume manufacturing we believe that this approach is viable for industrial deployment.

In the following sections we will present the design of the wedge using FDTD simulations, the mold fabrication by FIB etching, the imprint replication of the wedges, and the optical measurements of the device.

## 2. DESIGN

The numeric calculations for this design were performed by FDTD in the software package Omnismim. The refractive polymer element was placed on top of a previously designed grating coupler with 20 rectangular slits of 315 nm wide and 70 nm deep, spaced by 315 nm. This coupler is etched in a 220 nm thick silicon layer on top of a 2  $\mu\text{m}$  thick oxide buffer layer. All simulations were performed in 2D, which is a good approximation for the 10  $\mu\text{m}$  wide waveguides used in the experiments.

In a first step we have calculated the angle under which 1.55  $\mu\text{m}$  light couples out of the silicon waveguide if the grating is completely covered with polymer (refractive index 1.506 of PAK polymer from Toyo Gosei Co.): 8.6° relative to the surface normal. This angle is different from the originally designed 10° due to the altered effective index of the optical mode.

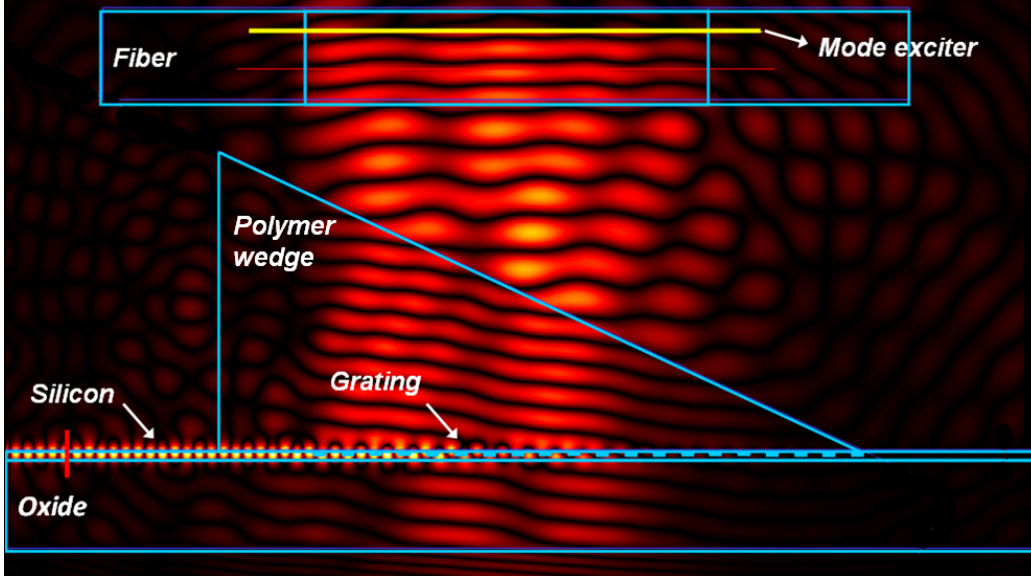


Figure 3. FDTD simulation of the polymer wedge with an angle of 24.7°.

In a second step we have manually calculated the angle  $\theta_i$  (see Fig. 2) by solving the equation  $\theta_i - \theta_t = 8.6^\circ$  and Snell's law. After some manipulations one obtains  $\theta_i = 24.7^\circ$ . This design was verified with FDTD in Omnismim, as depicted in Fig. 3. In this picture the mode is excited from the fiber; this setup was used to calculate the power fraction that is coupled between fiber and silicon waveguide. For a standard grating coupler with fiber positioned at  $10^\circ$  off-normal the obtained coupling efficiency is 43%; with the setup as depicted in Fig. 3 (wedge angle  $24.7^\circ$ ) the coupling efficiency is 49% (both simulations were done with a grid size of 15 nm). This means that theoretically we expect a small increase in efficiency. We have verified this with a calculation of Fresnel's equations, and found that the insertion of a polymer wedge in principle reduces the power reflection of a vertically incident plane wave from 30% to 20%. This increase is somewhat compensated by a decrease of the grating efficiency due to a different angle and index contrast.

To estimate the amount of reflected light we have performed a simulation with mode excitation in the silicon waveguide. Fig. 4 shows the power fraction coupled upwards (without taking fiber mode overlap into account), downwards into the substrate, back into the waveguide, and through the grating. Reflections are below -12 dB for wavelengths up to 1616 nm. However, it should be noted that the expected experimental reflections are lower, because scattered light in the wedge creates a noise background during the simulation. By artificially shielding the detector with a thin gold stripe we have obtained a reflection lower than -20 dB. This reflection can in principle be reduced by designing the grating couplers for operation at off-normal angles greater than  $10^\circ$ .

### 3. FABRICATION

#### 3.1 Mold fabrication by FIB

The general fabrication scheme (as presented in Fig. 5) involves a number of steps that will be discussed in more detail in the following.

Firstly, a mold for imprinting a structure in UV curable polymer on silicon is necessarily transparent to UV radiation, so we have chosen a quartz substrate. However, to avoid charging problems during FIB etching of the wedge molds the quartz substrate was first covered with a 100 nm layer of Ti that was electrically connected to the sample stage in the FIB vacuum chamber during etching. Optical lithography and liftoff of the Ti was performed to define the locations of the wedges and to print alignment structures for the imprint lithography. An electron micrograph after this first step is displayed in Fig. 6, where the white arrow indicates where an array of wedges will be etched.

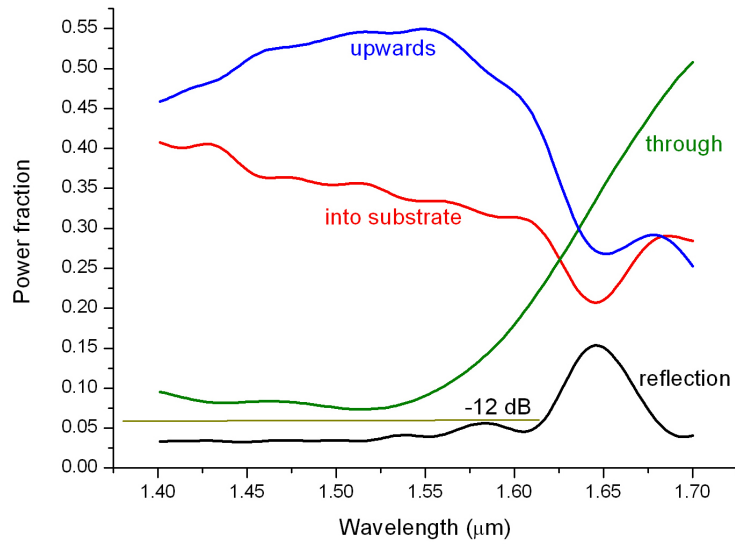


Figure 4. By mode excitation from the silicon waveguide we have calculated the power fractions coupled upwards, downwards into the substrate, back into the waveguide, and through the grating coupler.

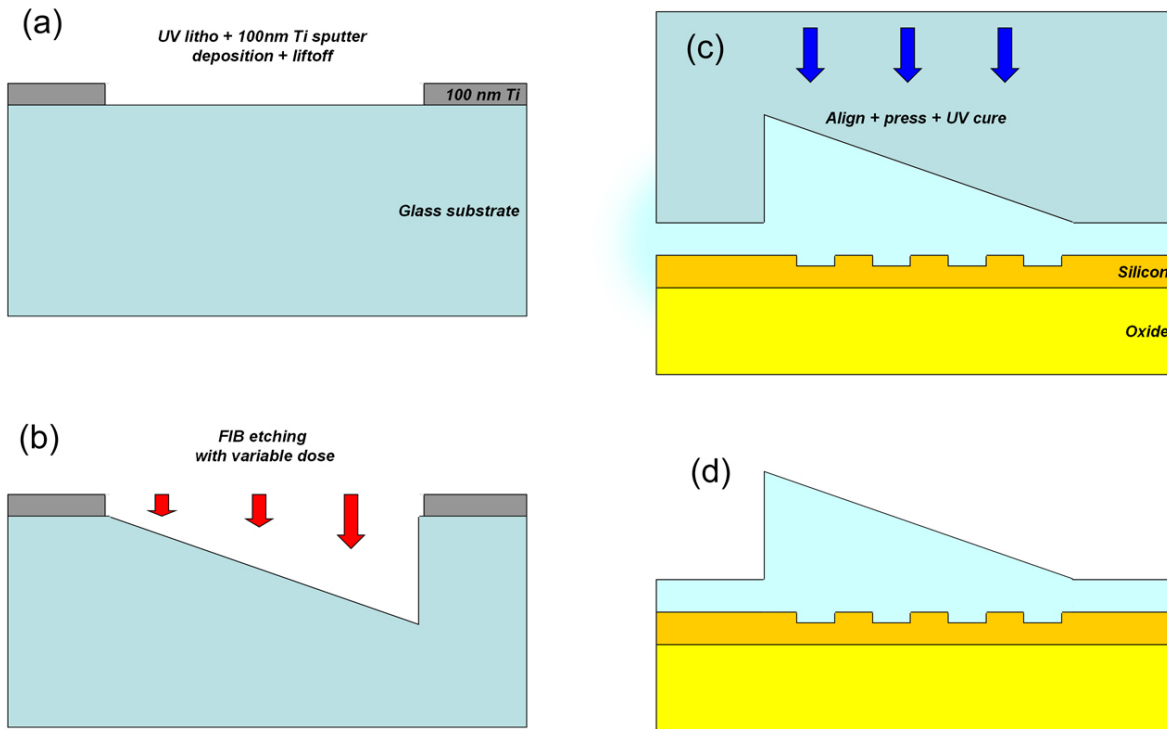


Figure 5. Schematic overview of the wedge fabrication procedure: (a) definition of wedge locations by optical lithography; (b) FIB etching of the wedges; (c) imprint of the wedges and curing with UV; (d) the final wedge after mold removal.

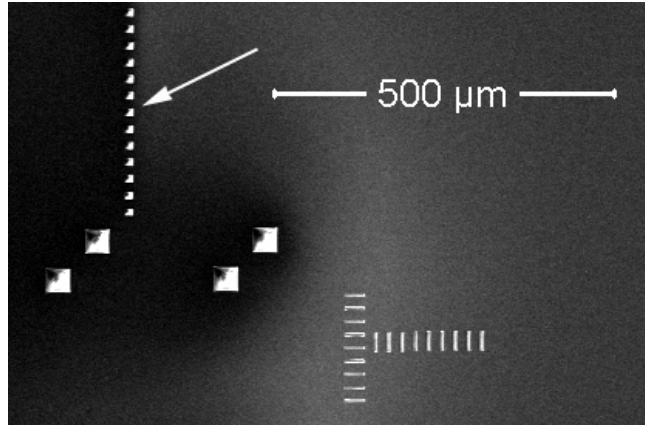


Figure 6. Overview of the patterned Ti layer on the quartz mold. The negative wedges will be defined in the squares indicated by the arrow. The other structures are meant for alignment during imprinting.

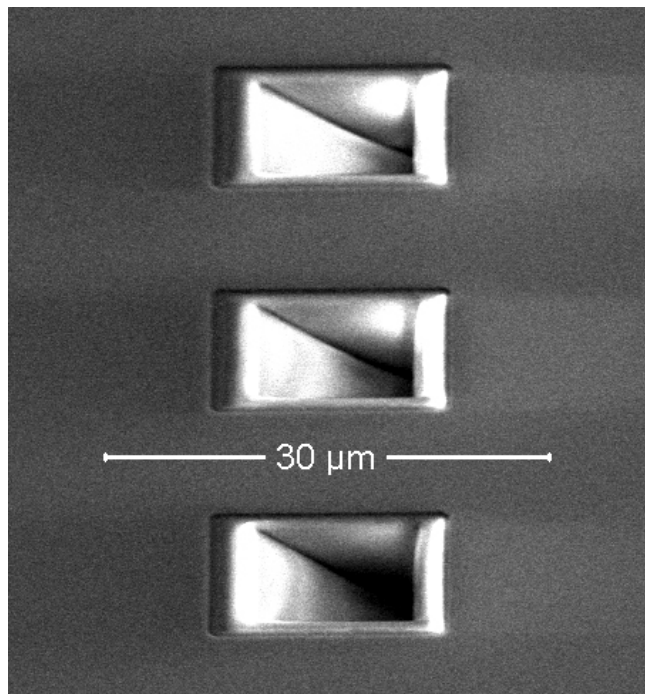


Figure 7. The negative wedges were etched after an image recognition scan and automated alignment.

In a second step the negative wedges were etched with FIB at normal incidence (FEI Nova Nanolab 600 with Raith pattern generator, 7 nA, 30 keV). Image recognition was used to align and etch 60 wedges in an automated way (about 15 minutes per wedge). Three of these wedges are presented in Fig. 7. The precisely angled and smooth bottom of the wedge molds was obtained by varying the dose in the etched rectangle. The mask consists of an array of 160 lines, 100 nm apart and 14  $\mu\text{m}$  long. These are scanned digitally, with a step size of 200 nm and a varying dwell time (from 1.2  $\text{mC}/\text{cm}^2$  to 30.965  $\text{mC}/\text{cm}^2$  with a step of 0.1872  $\text{mC}/\text{cm}^2$ ). This procedure was repeated 60 times; so the dose of the deepest line was 1.86  $\text{C}/\text{cm}^2$ . Optimization of this procedure was performed by cross-sectional inspection and iteration. We have found that the angled etch pit bottom (the optically smooth refraction plane) is no longer planar when the largest available beam current of 20 nA is used, which is most likely caused by a lesser beam quality. We have also experimented with larger wedge angles and found that angles larger than about 45° could not be obtained with smooth refraction planes. In this case we have observed the formation of ripples.

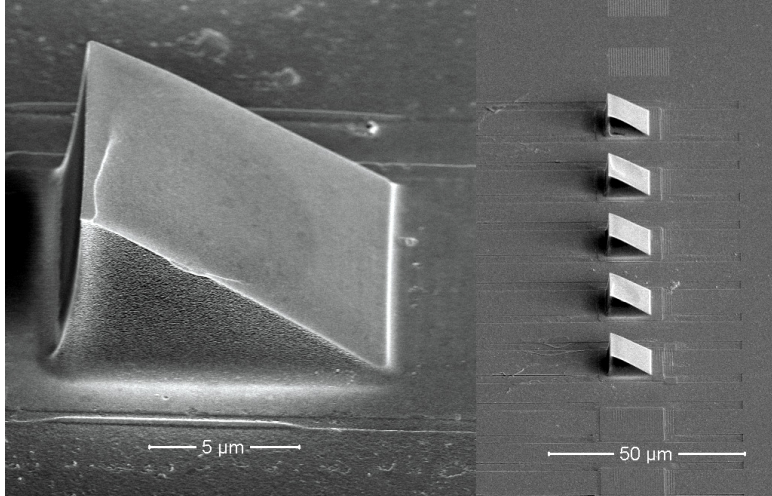


Figure 8. Micrographs of fabricated polymer wedges covered with a thin layer of gold to avoid charging. Note the smoothness of the refractive plane.

Although FIB fabrication of a mold inherently avoids the problems of optical losses, these can still be detrimental when a transparent mold is used. If too much losses (for UV transmission) would be introduced by the etch procedure, exposure would become difficult. However, we have observed no effects of this kind. No specific transmission measurements were performed, but by microscopic inspection of the mask during alignment no noticeable darkening (for visible light) was observed.

### 3.2 Wedge fabrication by imprint

After the wedge etching the quartz mold was prepared for imprinting by performing an anti-adhesive treatment. For a first generation of wedges the patterned Ti layer and the negative wedges were first covered with a 100 nm thick layer of silica by plasma deposition. Then the mold was immersed in (tridecafluoro-1,1,2,2-tetrahydrooctyl) trichlorosilane ( $C_8H_4Cl_3F_{13}Si$ , ABCR GmbH) in pentane solution (0.1%) and subsequently rinsed using acetone, isopropyl alcohol, and deionized water. The thin deposited silica layer was necessary because this anti-adhesive treatment is designed for silicon oxide. An extra anticipated advantage of the patterned Ti layer is that, as the UV exposure does not penetrate the Ti layer, regions in between wedges are not exposed. This eliminates the residual layer. However, we have found that in this case the wedges are easily released from the silicon during mold removal or subsequent rinsing. In a later generation the yield was greatly increased by completely removing the Ti layer (in diluted HF) and doing the anti-adhesive treatment directly on the quartz. This leaves behind a residual layer with a thickness that depends on the applied pressure and the viscosity of the polymer.

Two different UV curable polymers were used: PAK (PAK-01 from Toyo Gosei Co. Ltd.) and SU8 (SU8-10 from MicroChem). Both were dispensed on the sample prior to alignment and pressing of the mold, and then UV exposed (performed on Karl Suss MA6 mask aligner). The SU8 resist is more viscous so a thicker residual layer can be expected. After mask removal the samples were flood exposed under a UV fiber lamp for 5 minutes. Some SEM micrographs (after deposition of a thin gold layer) are presented in Fig. 8. Note the smoothness of the refractive plane.

## 4. MEASUREMENT

To determine the coupling efficiency of the fabricated coupling structure we have used a fiber-to-fiber transmission measurement for TE polarized light from a super luminescent LED. The structure consisted of two shallow input coupler fabricated with optical lithography and polymer wedges. In the integrated circuit the light is guided by a straight  $10\ \mu m$  wide waveguide and tapered down to a wire with approximate width of 500 nm. First a reference measurement was performed on gratings without polymer wedge, with both fibers positioned nearly vertically (at an angle of  $10^\circ$ ). Then, the fibers were tilted to a perfectly normal position and positioned above the gratings

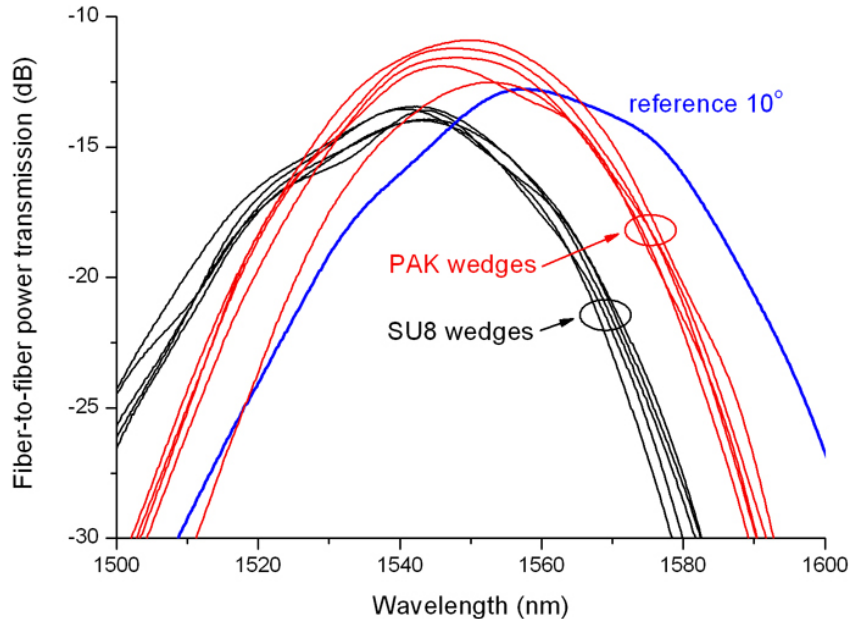


Figure 9. Fiber-to-fiber power transmission for 5 wedge pairs on two different samples.

with polymer wedges. The measurements were performed on the second generation of wedges, where the Ti layer was removed from the mask and thus a residual polymer layer covers the waveguides. Two different samples were fabricated, one with PAK and one with SU8 polymer. Fig. 9 depicts the measured fiber-to-fiber coupling efficiencies for 5 different wedge pairs on both samples. Coupling with near-vertical fibers causes a loss of about 13 dB, i.e. about 6.5 dB per coupler, which is equivalent to what was reported before. The vertically positioned fibers above the PAK wedges have a slightly higher coupling efficiency, 5-6 dB per coupler. This increase in efficiency is supported by the simulations in section 2. The SU8 wedges, on the other hand, show a somewhat lower efficiency. This can be attributed to a thicker residual layer (due to the higher viscosity) and possibly due to some misalignment. Nevertheless, from these results it is clear that the angled refractive planes have a good optical quality (as visible in Fig. 8). This proves the ability of FIB milling of optically smooth structures in quartz.

These polymer wedges enable flip-chip bonding of vertically emitting lasers. However, this process requires a thermal cycle of typically between 240 and 300°C. To assess the thermal stability of the two polymers we have therefore baked both samples for 5 minutes at 300°C on a hotplate in air. Afterwards the fiber-to-fiber transmission was measured again (this time with a tunable laser), as depicted in Fig. 10. The PAK polymer wedges show a significant decrease of efficiency, although the value does not drop below that of the reference couplers. The SU8 wedges show no decrease in efficiency. We can therefore conclude that SU8 polymer shows a better thermal stability, but to obtain a higher efficiency with SU8 wedges they have to be fabricated with SU8 of lower viscosity, which can be obtained by mixing with an appropriate solvent.

## 5. CONCLUSIONS

We have successfully designed, fabricated and measured polymer wedges that enable perfectly vertical coupling to a silicon photonic integrated circuit. The wedges were fabricated by imprinting a UV curable polymer with a focused-ion-beam fabricated mold with 3D geometry. The devices were submitted to a thermal treatment at 300°C to verify the applicability of this procedure for flip-chip soldering of vertical cavity lasers. The measurement results support that there is no coupling efficiency penalty when the correct polymer is chosen. The presented results prove the applicability of FIB for the fabrication of imprint molds with 3D geometry.

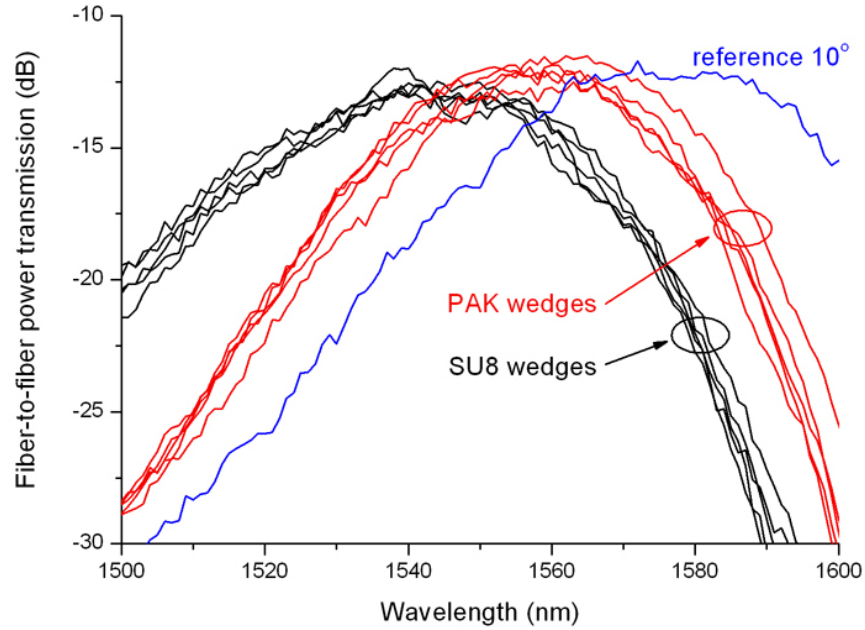


Figure 10. After a thermal cycle at 300°C the PAK polymer shows a slight decrease of efficiency; SU8 is stable.

## REFERENCES

- [1] Taillaert, D., Bienstman, P., and Baets, R., "Compact efficient broadband grating coupler for silicon-on-insulator waveguides," *Optics Letters* **29**(23), 2749–2751 (2004).
- [2] Van Laere, F., Ayre, M., Taillaert, D., Van Thourhout, D., Krauss, T. F., and Baets, R., "Compact and efficient fibre-to-waveguide grating couplers in inp-membrane," *Electronics Letters* **42**(6), 343–345 (2006).
- [3] Roelkens, G., Van Thourhout, D., and Baets, R., "High efficiency silicon-on-insulator grating coupler based on a poly-silicon overlay," *Optics Express* **14**(24), 11622–11630 (2006).
- [4] Schrauwen, J., Van Laere, F., Van Thourhout, D., and Baets, R., "Focused-ion-beam fabrication of slanted grating couplers in silicon-on-insulator waveguides," *IEEE Photonics Technology Letters* **19**(9-12), 816–818 (2007).
- [5] Van Laere, F., Claes, T., Schrauwen, J., Scheerlinck, S., Bogaerts, W., Taillaert, D., O’Faolain, L., Van Thourhout, D., and Baets, R., "Compact focusing grating couplers for silicon-on-insulator integrated circuits," *IEEE Photonics Technology Letters* **19**(21-24), 1919–1921 (2007).
- [6] Roelkens, G., Van Thourhout, D., and Baets, R., "High efficiency grating coupler between silicon-on-insulator waveguides and perfectly vertical optical fibers," *Optics Letters* **32**(11), 1495–1497 (2007).